

ARES Upgrade for Super-KEKB

Tetsuo Abe

KEK, Tsukuba, Ibaraki 305-0801, Japan

ARES is a normal-conducting RF accelerating cavity system for KEKB, which has been successfully operated to store the high-current beams. Aiming at luminosity frontiers beyond $10^{35}\text{cm}^{-2}\text{s}^{-1}$, an upgrade project toward Super-KEKB is being proposed, where about four times more beam currents are to be stored and supported by the RF system. In this report, upgrade items relevant to the ARES system are reviewed and discussed.

1. INTRODUCTION

The ARES¹ system [1], which is a normal-conducting RF accelerating cavity system for the double-ring asymmetric-energy e^+e^- collider: KEKB [2], consists of three components: a HOM-damped Accelerating Cavity (AC), an energy-Storage Cavity (SC) with TE₀₁₃ mode and a Coupling Cavity (CC) to connect AC with SC. The schematic drawing of the three-cavity system is shown in Figure 1. The field in AC is electromagnetically coupled, via CC, with that in the large cylindrical SC with a high- Q value.

The three-cavity system has in principle three fundamental modes due to the coupled oscillation with three oscillators. In case of ARES, the $\pi/2$ mode² is adopted as an accelerating mode, where the coupling factors are related to the ratio of stored energies in cavities according to the equivalent circuit model [3],

$$U_s/U_a = k_a^2/k_s^2, \quad (1)$$

where U_s and U_a indicate energies stored in SC and AC respectively, k_a is a coupling factor between AC and CC, and k_s between SC and CC. The operation with the $\pi/2$ mode has strong advantage that the field of this mode is the most stable against heavy beam loadings and detunings [3]. Especially, the amount of detuning for the $\pi/2$ mode is reduced according to the following formula,

$$\Delta f_{\pi/2} = \frac{\Delta f_a}{1 + U_s/U_a}, \quad (2)$$

if the energy ratio U_s/U_a is large enough. In the above formula, Δf_a indicates an amount of the optimum detuning for AC, and $\Delta f_{\pi/2}$ is a corresponding amount of detuning for the accelerating $\pi/2$ mode. The current value of U_s/U_a is 9. Another advantage of the $\pi/2$ -mode operation is that the parasitic 0 and π modes can be damped selectively out of CC, where there is basically no field of the $\pi/2$ mode in CC.

¹ARES stands for Accelerator Resonantly coupled with Energy Storage.

²Phase difference of oscillations in between neighboring cavities is $\pi/2$.

Total cavity voltage	8.0 MV
Maximum beam current	~ 1.8 A
RF input power	~ 300 kW /cavity
HOM power	$> \sim 5$ kW /cavity
Trip rate	~ 1 /cavity/3 months

Table I Summary of the recent operation status of the 20 ARES cavities in LER (April \sim June, 2003).

The recent operation status, in April \sim June, 2003, is summarized in Table I. The 20 ARES cavities in LER³ together with the 10 cavities in HER⁴ have been successfully operated to store the recent high-current beams of KEKB stably.

An upgrade of KEKB, Super-KEKB project, is being proposed aiming at luminosity frontiers beyond $10^{35}\text{cm}^{-2}\text{s}^{-1}$, where the design beam currents of LER and HER are 9.4 A and 4.1 A respectively. From the operational performance so far, we will be able to manage with the design current of 4.1 A in Super-KEKB HER using the current version of ARES cavities, while we have to have measures on Super-KEKB LER against the larger detuning, higher HOM power, and higher RF input power, which will be discussed in the following sections.

2. ENERGY-RATIO ISSUE

Due to the heavier beam loading in Super-KEKB LER, the detuning for AC will be needed to be increased into -710 kHz from -200 kHz in KEKB. Therefore, the detuning for the accelerating $\pi/2$ mode will be comparable with the revolution frequency of 99.4 kHz if the energy ratio U_s/U_a is unchanged. Against the larger detuning, we will increase the energy ratio from 9 to 15.

³LER stands for Low Energy Ring.

⁴HER stands for High Energy Ring.

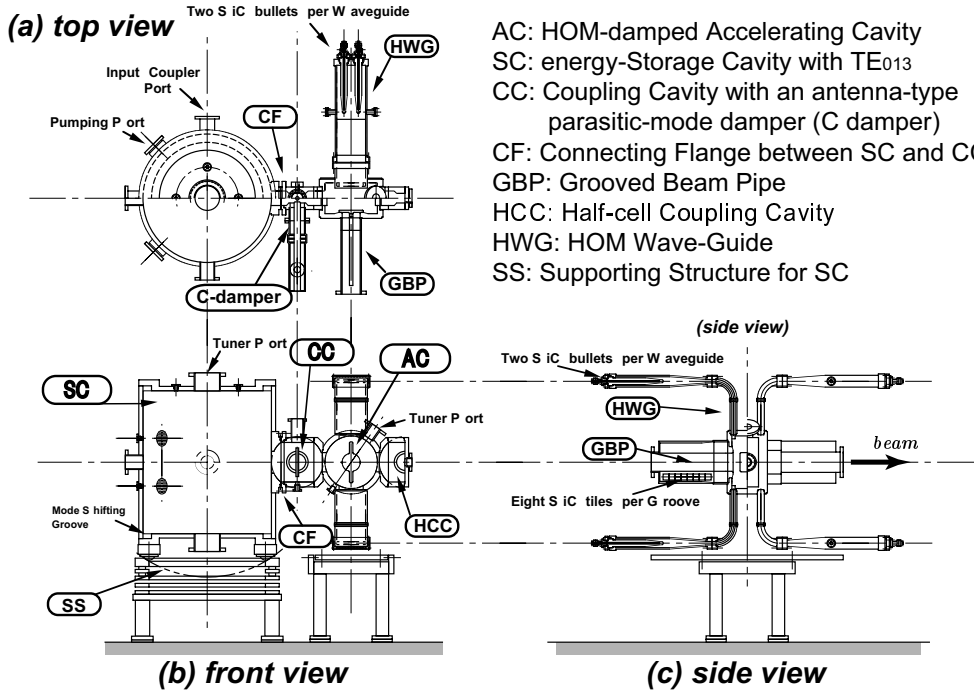


Figure 1: A schematic drawing of the three-cavity system ARES. (a) The top view, (b) front view perpendicular to the beam axis, and (c) side view parallel to the beam axis.

2.1. Modification of the AC's design

The energy ratio is also related to the external Q values as follows, applying the Slater's tuning curve [4],

$$U_s/U_a = Q_{ext,s}/Q_{ext,a} , \quad (3)$$

where $Q_{ext,s}$ and $Q_{ext,a}$ indicate external Q values of SC and AC respectively. Therefore, the energy ratio can be changed by changing the size of the rectangular aperture between AC and CC or between SC and CC. We modify the design of the aperture between AC and CC, not between SC and CC, because we also have to upgrade the HOM loads in AC on which CC is brazed, and we could re-use the current version of SC.

Numerical values of $Q_{ext,a}$ are calculated using HFSS as a function of the aperture size, where the width of the aperture is fixed at the current design value of 120 mm, and only the height (h) is floated. Energy ratios are estimated from the calculated $Q_{ext,a}$ values according to the formula (3). The result is shown in Figure 2. For $U_s/U_a = 15$, we have to increase the window height from 160 mm to 175 mm. This modification is acceptable from a point of view of the mechanical structure of ARES.

As a result from the larger energy ratio, the wall loss in SC becomes large, from ~ 100 kW in KEKB to ~ 150 kW in Super-KEKB. However, continuous stable operations with high wall-loss powers over 200 kW have been verified in the new ARES test-stand (See section 4.).

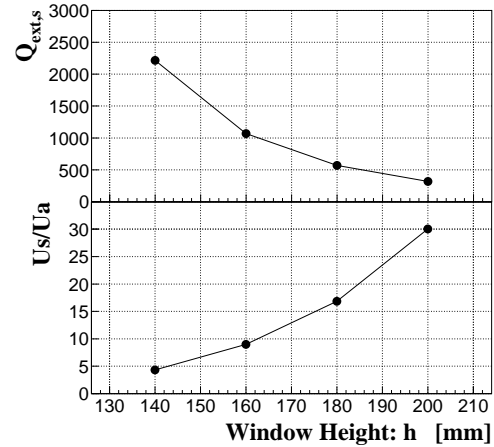


Figure 2: External Q values of AC (top) and the energy ratios (bottom) as a function of the window height of the aperture.

2.2. Instabilities

We have to consider longitudinal coupled-bunch instabilities (CBIs) driven by the following two sources, the $\pi/2$ mode, and the parasitic 0 and π modes.

Figure 3 shows the real part of the longitudinal impedance per cavity of the $\pi/2$ mode for Super-KEKB LER. Increasing the energy ratio reduces the amount of the detuning significantly. Figure 4 shows

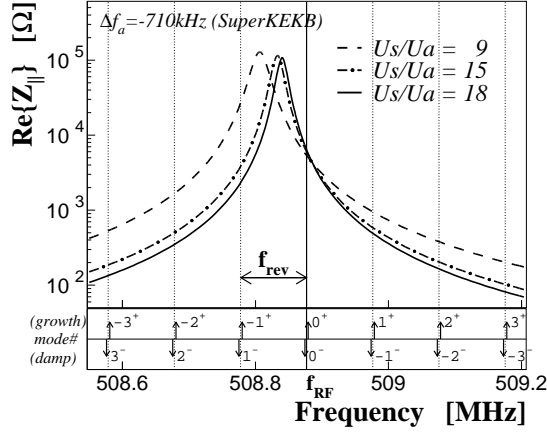


Figure 3: Real part of the longitudinal impedance per cavity of the $\pi/2$ mode for $U_s/U_a = 9$ (dashed line), $U_s/U_a = 15$ (dashed-dotted line), and $U_s/U_a = 18$ (solid line) for Super-KEKB LER. f_{RF} and f_{rev} indicates the RF and revolution frequencies respectively.

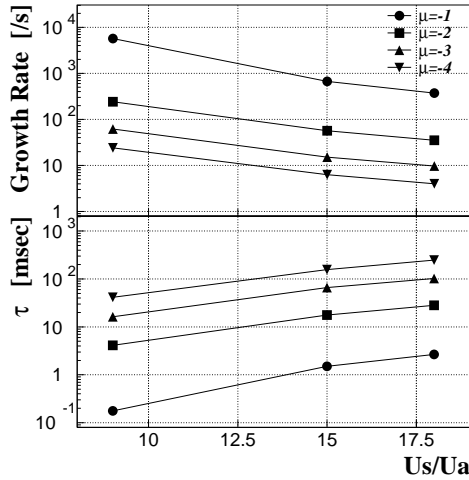


Figure 4: Growth rates (top) and times (bottom) of the $\pi/2$ -mode CBI for the four lowest modes: $\mu = -1, -2, -3, -4$ as a function of the energy ratio.

the growth rates, or growth times, of the CBI for each case. Here we assume Super-KEKB LER current of 9.4 A which is supported by ARES 28 cavities with a cavity voltage of 0.5 MV/cavity. Increasing the energy ratio eases the $\mu = -1$ CBI by one order of magnitude in the growth rate, down to a manageable level, $\tau \sim 1.5$ msec, within the RF system. Not only the $\mu = -1$ CBI but also the $\mu = -2$ one might be needed to be managed since the radiation damping time in SuperKEKB LER will be ~ 30 msec.

The second source of CBI is the parasitic 0 and π modes which have a symmetric impedance distribution with respect to the RF frequency, i.e. the

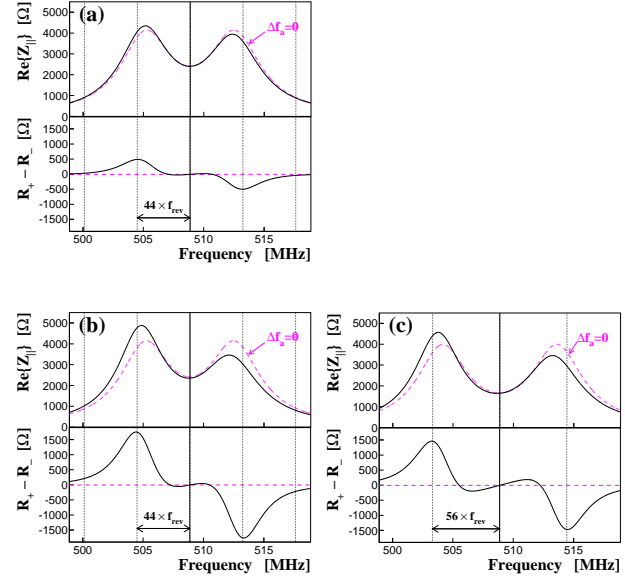


Figure 5: Real parts of the longitudinal impedances per cavity (top) and their asymmetries with respect to the RF frequency (bottom) of the parasitic 0 and π modes for (a) $\Delta f_a = -200$ kHz with $U_s/U_a = 9$ (KEKB), (b) $\Delta f_a = -710$ kHz with $U_s/U_a = 9$ (Super-KEKB), and (c) $\Delta f_a = -710$ kHz with $U_s/U_a = 15$ (Super-KEKB), where the dashed lines indicate impedances in case of no detuning. f_{rev} indicates the revolution frequency.

impedance contributions from the two modes balance between exciting and damping terms of the CBI, in case of no detuning ($\Delta f_a = 0$), as shown in Figure 5. However, the fields of those modes are subject to the first order perturbation of tuning errors. When AC is detuned, the first order term of the perturbation is proportional to $\Delta f_a / (f_\pi - f_0)$, where f_0 and f_π indicate the frequencies of the 0 and π modes respectively, and the impedance contributions from the two modes cannot balance any more. For KEKB with $\Delta f_a = -200$ kHz, the asymmetry is so small, as shown in Figure 5-(a), that the maximum growth time is ~ 46 msec, which is slower than the radiation damping time of ~ 23 msec. However, for the Super-KEKB LER, the asymmetry becomes larger as shown in Figure 5-(b) with $U_s/U_a = 9$. In this case, the fastest growth time is ~ 3.3 msec. Even if the energy ratio is increased into 15, the fastest growth time is ~ 4.0 msec, still much faster than the radiation damping time.

The growth time of the CBI driven by the parasitic modes is comparable with that by the HOMs, so that we will need some bunch-by-bunch longitudinal feedback system in any case to suppress the broad-band CBI with $\tau \sim$ several msec.

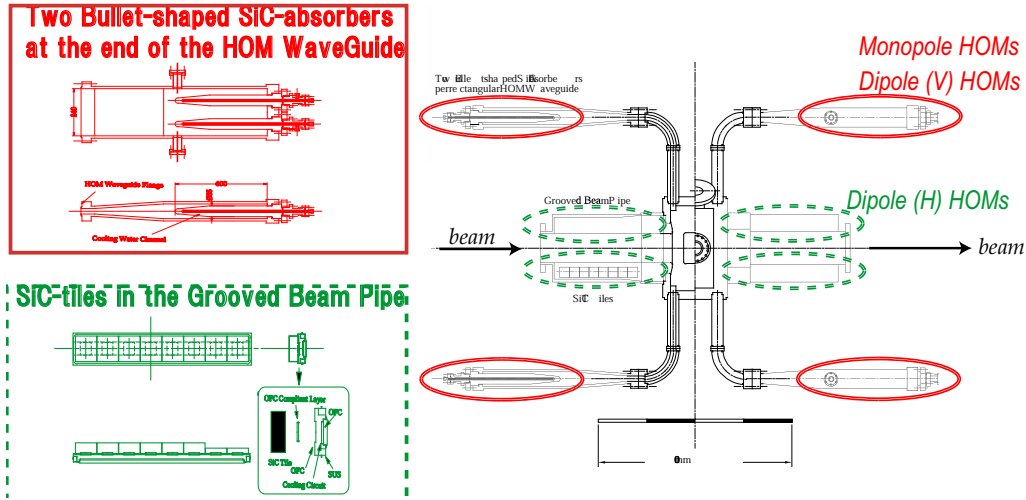


Figure 6: HOM absorbers of the ARES damped structure.

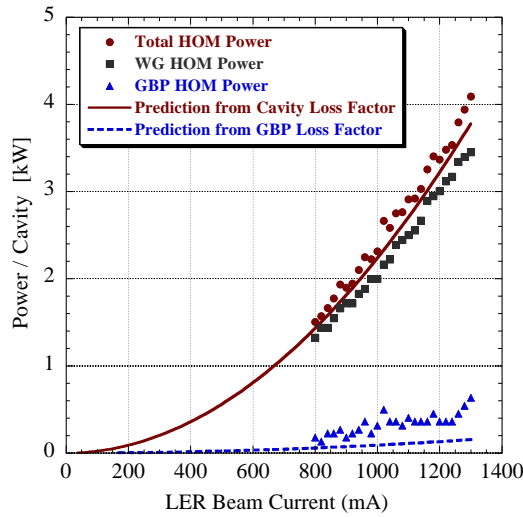


Figure 7: Comparisons of the current HOM powers between the measurements (plots) and predictions (lines) as a function of the LER beam current.

3. HOM-LOAD ISSUE

The ARES system has a damped structure with two types of HOM absorbers [5]. One of them is a set of two bullet-shaped SiC loads attached at the end of the rectangular HOM waveguide (WG), and the other is a set of eight SiC tiles attached on the inner surface of the grooved beam pipe (GBP) [6]. One AC has four sets of WG HOM absorbers and four sets of GBP ones, as shown in Figure 6.

The WG HOM loads are directly water-cooled and absorb the monopole and vertically polarized dipole HOMs. High power tests were done for the loads using a 1.3 GHz CW klystron, and it was verified that one bullet could absorb up to 3.3 kW (26.4 kW per cavity)

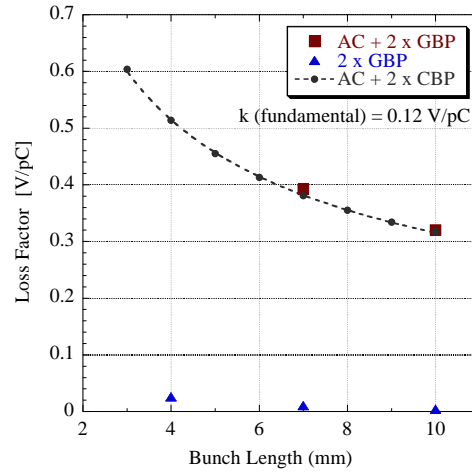


Figure 8: Comparisons of the HOM loss factors as a function of the bunch length between the 3D-MAFIA (squares) and 2D-ABCI (circles) predictions.

without any problem. This limit was only due to the maximum power stably supplied by the klystron.

The GBP HOM loads are brazed on a water-cooled copper plate and absorb the horizontally polarized dipole HOMs. High power tests were also done for the loads using the same klystron up to 0.5 kW per groove (2.0 kW per cavity).

Figure 7 shows comparisons of the current HOM powers per cavity as a function of the LER beam current between the measurements (plots) and predictions (lines) for the current KEKB LER with 1224 bunches (four-bucket spacing) and bunch length (σ_z) of 7 mm. The predictions were made using 3D-MAFIA. The total HOM-power measurements are reproduced by the predictions fairly well.

Figure 8 shows comparisons of the HOM loss factors as a function of the bunch length between the 3D-

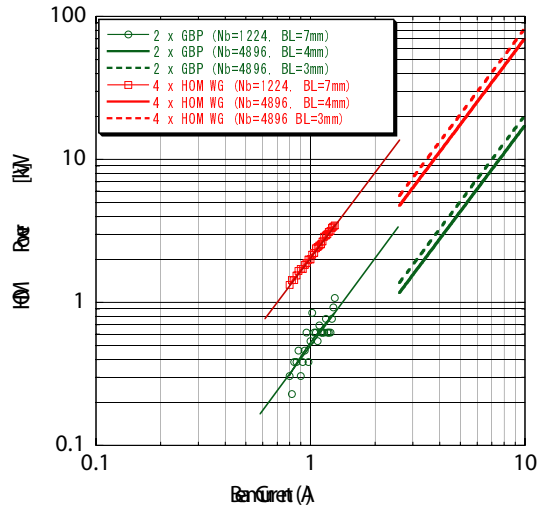


Figure 9: HOM-power extrapolation from KEKB to Super-KEKB. The circles indicate the measurements in KEKB with 1224 bunches (four-bucket spacing) and $\sigma_z = 7$ mm. The lines above 2.6 A are predictions for Super-KEKB LER with 4896 bunches and $\sigma = 3$ mm (dashed lines) or $\sigma = 4$ mm (bold solid lines).

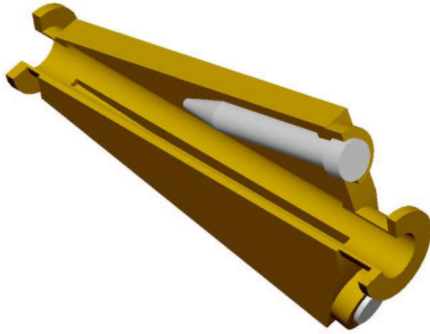


Figure 10: Winged chamber loaded with directly water-cooled SiC absorbers, used in the movable-mask sections of KEKB.

MAFIA and 2D-ABCI predictions. Since the agreement is well for $\sigma_z = 7$ mm and 10 mm, we use 2D-ABCI predictions for $\sigma_z = 3 \sim 4$ mm to be achieved in Super-KEKB, for which one cannot use 3D-MAFIA due to a too large number of meshes.

We can extrapolate the current HOM powers to those in Super-KEKB LER with 4896 bunches and $\sigma = 3$ mm. In Figure 9, the current HOM powers are shown as a function of the LER beam current under the KEKB-LER design current of 2.6 A, and the extrapolated (or expected) HOM powers are shown above 2.6 A based on the 2D-ABCI simulation. The dashed lines indicate the expected maximum HOM powers with $\sigma_z = 3$ mm. The expected HOM power in the WG loads is 80 kW per cavity, whereas the limit verified in the high power test is 26.4 kW per cavity. We could manage this higher power by increas-

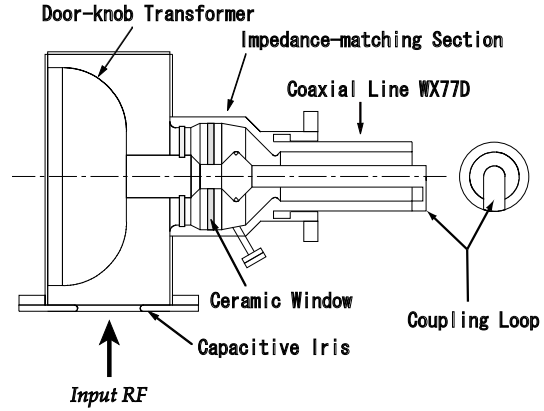


Figure 11: A schematic drawing of the input coupler for the ARES system.

ing the number of absorbers per WG, and introducing an enhanced water cooling, depending on results from the high power test to be resumed soon. The expected HOM power in the GBP loads is 20 kW per cavity, whereas the verified limit is 2 kW per cavity. We might have to adopt a new type of a HOM absorber, for example, the winged chamber loaded with directly water-cooled SiC absorbers like seen in Figure 10. This type of absorbers has been already developed in collaboration between the KEKB vacuum and ARES groups, and several chambers have been installed to absorb the HOM power from the movable masks [7].

4. COUPLER ISSUE

A schematic drawing of the ARES input coupler [8] is shown in Figure 11. RF input power coming through a rectangular waveguide WR1500 is fed, via the doorknob transition with a capacitive iris at the entrance, into the the coaxial line WX152D with a disk-type ceramic window which separates vacuum and atmosphere. This coaxial line is over- and under-cut for impedance matching, and connected, via a taper section, to another coaxial line WX77D, the end of which is terminated with a magnetic coupling loop. The design capability is 400 kW at maximum for KEKB, and needs to be increased up to 800 kW for Super-KEKB.

In advance of the coupler mass production, prototype couplers were tested up to 950 kW at a test bench where two couplers were combined with their coupling loops put face-to-face and electromagnetically coupled with each other in a two-port cylindrical vacuum chamber. RF power was fed into one of the couplers, and the other was connected to a 1 MW dummy load. The verified limit of 950 kW is high enough for Super-KEKB, however, the situation of the test bench

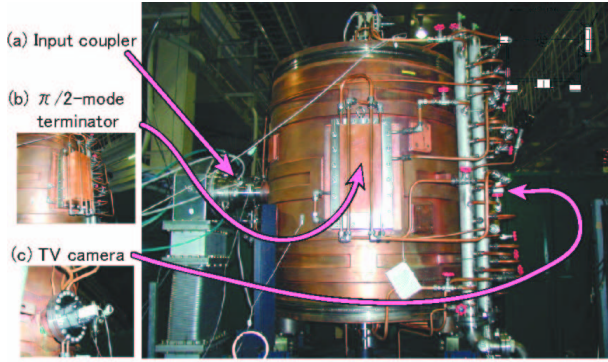


Figure 12: Pictures of the new coupler test-stand. (a) The input coupler, (b) $\pi/2$ -mode terminator, and (c) TV camera are attached to the large cylindrical SC seen in the center.

is not actual. The actual operating condition, where a coupler is attached to a large amount of electromagnetic energy stored in SC, is much severer than that in the high power test of the test bench.

For the purpose of ensuring the stable performance of the coupler for input powers up to 800 kW in the actual situation, we have started a new test-stand, where a coupler is attached to SC on which a $\pi/2$ -mode terminator is attached instead of CC and AC. In this configuration, the SC works as a dummy load. Figure 12 shows pictures of the test-stand. The important advantage of using the $\pi/2$ -mode terminator is that the operation is free from multipactoring-discharge phenomena in AC. The input power was raised up automatically by a computer, keeping the vacuum pressure below a specified level. Figure 13 shows a power history of the conditioning of the first coupler tested in this test-stand. We often observed multipactoring discharge inside the coaxial line WX77D in the range of input powers from 150 to 190 kW. This phenomena were accompanied by a vacuum-pressure rise. Figure 14 shows an example of the pictures of the discharge taken with a TV camera attached to the view port opposite to the coupler. This kind of discharge was also observed in the second coupler of the test-stand, and in some couplers used in the KEKB operation. In order to understand the phenomena and to take measures, simulation studies are ongoing.

5. Summary

For the luminosity upgrade of KEKB toward Super-KEKB, we need to increase the energy ratio U_s/U_a from 9 to 15 in order to reduce the larger detuning. The severest -1 -mode longitudinal CBI driven by the accelerating $\pi/2$ mode can be eased by one order of magnitude, down to a manageable level, $\tau = 1.5$ msec, within the RF feedback system. The imbalance of the parasitic 0 and π modes drives broad-band CBIs with

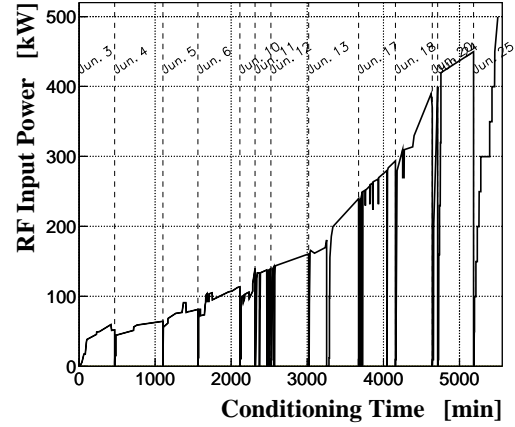


Figure 13: Power history of the conditioning.



Figure 14: An example of the pictures of the multipactoring discharge in the coaxial line WX77D of the coupler.

a growth time of several msec, which are to be suppressed with some bunch-by-bunch longitudinal feedback system. We have found no serious problems on the energy-ratio issue so far.

We also need a HOM-load upgrade for the WG and GBP loads up to ~ 80 kW and ~ 20 kW per cavity respectively. High power tests to manifest the real limits of the loads are to be resumed soon. In the current upgrade plan, we re-design the AC part only, so that SCs can be re-used.

We have started a new coupler test-stand with the actual condition, where a coupler is attached to SC on which a $\pi/2$ -mode terminator is attached instead of CC and AC. Multipactoring discharge phenomena were often observed in a certain input-power region, which are to be suppressed in Super-KEKB.

References

- [1] T. Kageyama *et al.*, "The ARES Cavity for KEKB", Prepared for International Workshop on Performance in Improvement of Electron-Positron

- Collider Particle Factories (e^+e^- Factories 99), Tsukuba, Japan, 21-24 Sep (1999).
- [2] K. Akai *et al.*, “Commissioning of KEKB”, Nucl. Instrum. Meth. A **499**, 191 (2003).
 - [3] Y. Yamazaki and T. Kageyama, Part. Accel. **44**, 107 (1994).
 - [4] J. C. Slater, “Microwave Electronics”, D. Van Nostrand, New York (1950).
 - [5] Y. Takeuchi *et al.*, “HOM Absorber for the ARES Cavity”, Proc. PAC97, Vancouver (1997).
 - [6] T. Kageyama, “Grooved Beam Pipe for Damping Dipole Modes in RF Cavities”, Proc. the 8th Symposium on Accelerator Science and Technology, 116 (1991).
 - [7] Y. Suetsugu *et al.*, “Development of Winged HOM Damper for Movable Mask in KEKB”, Proc. PAC2003, Portland (2003).
 - [8] F. Naito *et al.*, “The Input Coupler for the KEKB ARES Cavity”, Proc. APAC98, Tsukuba (1998).